Available online at www.sciencedirect.com

ScienceDirect

Current Opinion in Electrochemistry

Review Article

Metal–nitrogen coordination moieties in carbon for effective electrocatalytic reduction of oxygen

Qiming Liu[1], Qiaoxia Li[1,2] and Shaowei Chen[1]

Abstract

Oxygen reduction reaction is a critical process at the cathode of proton-exchange membrane fuel cells and metal–air batteries. Carbon-based single metal atom nanocomposites have emerged as effective alternatives to state-of-the-art platinum catalysts, in which the electrocatalytic activity is attributed largely to the formation of metal–nitrogen coordination moieties (MN_x) within the carbon matrix. In this review, we summarize recent progress in the studies of metal and nitrogen codoped carbon as single-atom catalysts toward oxygen reduction reaction within the context of the atomic configuration of the MN_x active sites and topologic characteristics of the carbon skeletons and include a perspective of the design and engineering of the nanocomposites for further enhancement of the electrocatalytic activity.

Addresses

[1] Department of Chemistry and Biochemistry, University of California, 1156 High Street, Santa Cruz, CA, 95064, USA

[2] Shanghai Key Laboratory of Materials Protection and Advanced Materials in Electric Power, College of Environmental and Chemical Engineering, Shanghai University of Electric Power, 2588 Changyang Road, Yangpu District, Shanghai, 200090, China

Corresponding authors: Chen, Shaowei (shaowei@ucsc.edu); Li, Qiaoxia (liqiaoxia@shiep.edu.cn)

Current Opinion in Electrochemistry 2020, **21**:46–54

This review comes from a themed issue on **Energy Storage**

Edited by **Mike Lyons** and **Kenneth I. Ozoemena**

For a complete overview see the Issue and the Editorial

Available online 15 January 2020

https://doi.org/10.1016/j.coelec.2020.01.002

Keywords

Oxygen reduction reaction, Metal-air battery, Fuel cell, Metal and nitrogen codoped, Carbon, Coordination moiety.

Proton-exchange membrane fuel cells and metal–air batteries represent two leading technologies for next-generation sustainable and clean energy conversion [1–4]. In these electrochemical systems, oxygen reduction reaction (ORR) at the cathode plays a critical role in determining the device performance, primarily because of the sluggish electron transfer kinetics and complex pathways of ORR. Platinum-based nanoparticles have been the catalyst of choice for ORR, yet the high cost and low natural abundance has severely hampered the widespread applications of the technologies [1,3–5]. Therefore, extensive research efforts have been devoted to the development of viable catalysts that are of low cost and high activity. Within this context, single (metal)-atom catalysts (SACs) have been attracting special attention, where the high atom utilization and maximal interactions with the supporting substrate render it possible to fundamentally optimize the catalytic efficiency and concurrently minimize the cost of the catalysts [2,6]. Among the various transition metals, SACs of Fe, Co, and Cu have shown remarkable ORR activity [2,4,6], which are mostly embedded within carbon matrices by taking advantage of carbon's low cost, high electrical conductivity, and ready manipulation of the electronic structures by deliberate doping with select heteroatoms. For instance, nitrogen is a commonly used dopant and can serve as effective binding sites to immobilize metal atoms forming M–N bonds [7]. In general, ORR occurs via two possible pathways, the direct pathway whereby oxygen undergoes four-electron reduction to water and the sequential pathway which involves the formation of hydrogen peroxide as an intermediate before the production of water [2,6]. Oxygen adsorption on SACs is in general argued to be the rate-determining step (RDS), in which a moderate adsorption is preferred for high-efficiency ORR [2]. In this review, we summarize recent progress of SACs involving Fe, Co, and Cu toward ORR, within the context of MN_x coordination configuration [8–11], nitrogen dopants [12–14], and carbon defects [15–19] and conclude with a perspective of the promises and challenges of SAC nanocomposites in ORR electrocatalysis.

Fe,N-codoped carbon SACs have been found to exhibit apparent activity toward ORR and can outperform state-of-the-art Pt/C in alkaline media [15–18]. This is mostly ascribed to the formation of the FeN_x moiety, in which the activity has been argued to be dependent on the x value. For example, in one recent study, Li et al. [8] prepared three FeN_xC_{4-x} samples (x = 1, 3, 4) by pyrolysis of N-doped carbon with Fe salts at increasing temperature and observed that the ORR activity decreased in the order of $FeN_4 > FeN_3C > FeN_1C_3$ both in acid and alkaline electrolytes, which is in good agreement with results from density functional theory (DFT) calculations in which the order of ORR activity was found to be $FeN_4 > FeN_3C > FeN_2C_2 > FeN_1C_3 >$

FeN_5. In fact, FeN_4 has been argued to be the ORR active sites in a large number of studies [12,13,20–22]. Yet in another study, Shen et al. [9] argued that FeN_2C_2 was more beneficial for ORR than FeN_4 both experimentally and theoretically, where, owing to the solvation effect, the DFT model of FeN_2C_2 was reconfigured with an additional dangling hydroxy ligand that was connected to the Fe center. Zhu et al. [10] also observed that FeN_2-type catalysts exhibited a competitive ORR performance with a half-wave potential ($E_{1/2}$) of +0.927 V vs. reversible hydrogen electrode (RHE) in alkaline media, and the catalysts even resisted the poisoning of SCN^- owing to the high affinity to O_2, which is in contrast to leading results in the literature. The fact that the ORR activity was accounted for by different FeN_x coordination structures in these studies suggests that other structural factors have to be included in the mechanistic discussion.

Several important questions arise. Will the activity vary when the metal center is coordinated to pyrrolic N and pyridinic N? In addition to the metal center, are the adjacent C and N atomic sites also active in ORR electrocatalysis? In one earlier study, Lu et al. [13] pyrolyzed tellurium nanowire@melamine formaldehyde polymer impregnated with Fe salts, and they observed that the obtained Fe–N–C materials exhibited an ORR activity comparable with that of Pt/C in 0.1 M KOH. DFT calculations of two types of FeN_4 (normal pyridine-type and Stone–Wales pyrrole-type FeN_4) showed that the Fe center of either FeN_4 was the predominant active site for ORR rather than the coordinated N atoms, and the C sites in the Stone–Wales FeN_4 could also contribute to the ORR activity, whereas in metal-free N-doped carbon, the ORR activity was relatively low owing to weak binding of oxygen species to the N and C sites. Yang et al. [20] reached a similar conclusion that the ORR activity originated from the synergistic interactions between the carbon sites and Fe center of the pyrrole-type Fe–N moieties. Taken together, these results suggest that in SACs, both the metal centers and

Figure 1

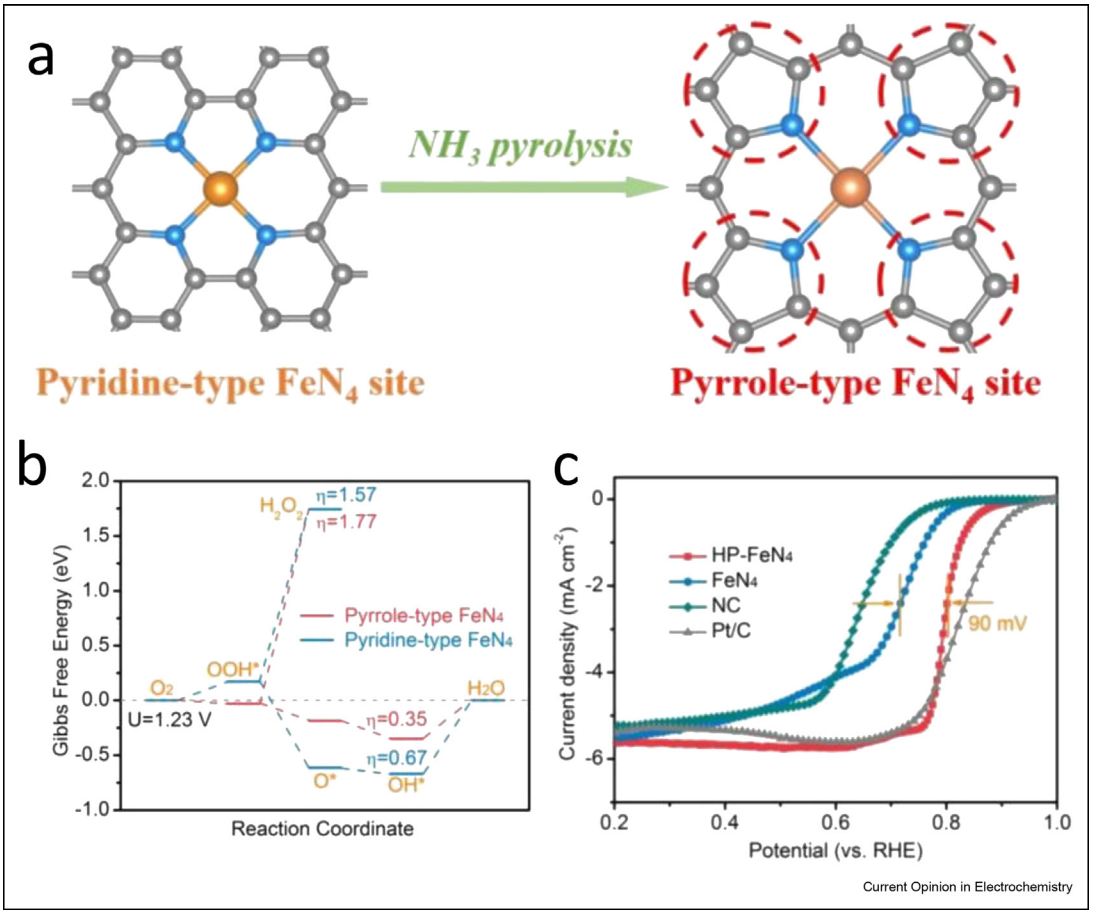

Configurational transformation of FeN4 sites in carbon and the impacts on ORR performance. **(a)** Preparation process of the high-purity pyrrole-type FeN_4 structure. The balls in gray, blue, and orange represent C, N, and Fe atoms, respectively. **(b)** Free energy diagram of the oxygen reduction reaction (ORR) on pyrrole-type FeN_4 and pyridine-type FeN_4. **(c)** ORR polarization curves of HP-FeN_4, FeN_4, and NC catalysts in O_2-saturated 0.5 M H_2SO_4 and 20% Pt/C in 0.1 M $HClO_4$ at the rotating rate of 1600 rpm. Reprinted with permission from Zhang et al. [12••] © 2020 Royal Society of Chemistry. RHE, reversible hydrogen electrode; HP-FeN4, high-purity pyrrol-type FeN4; NC, nitrogen-doped carbon.

Figure 2

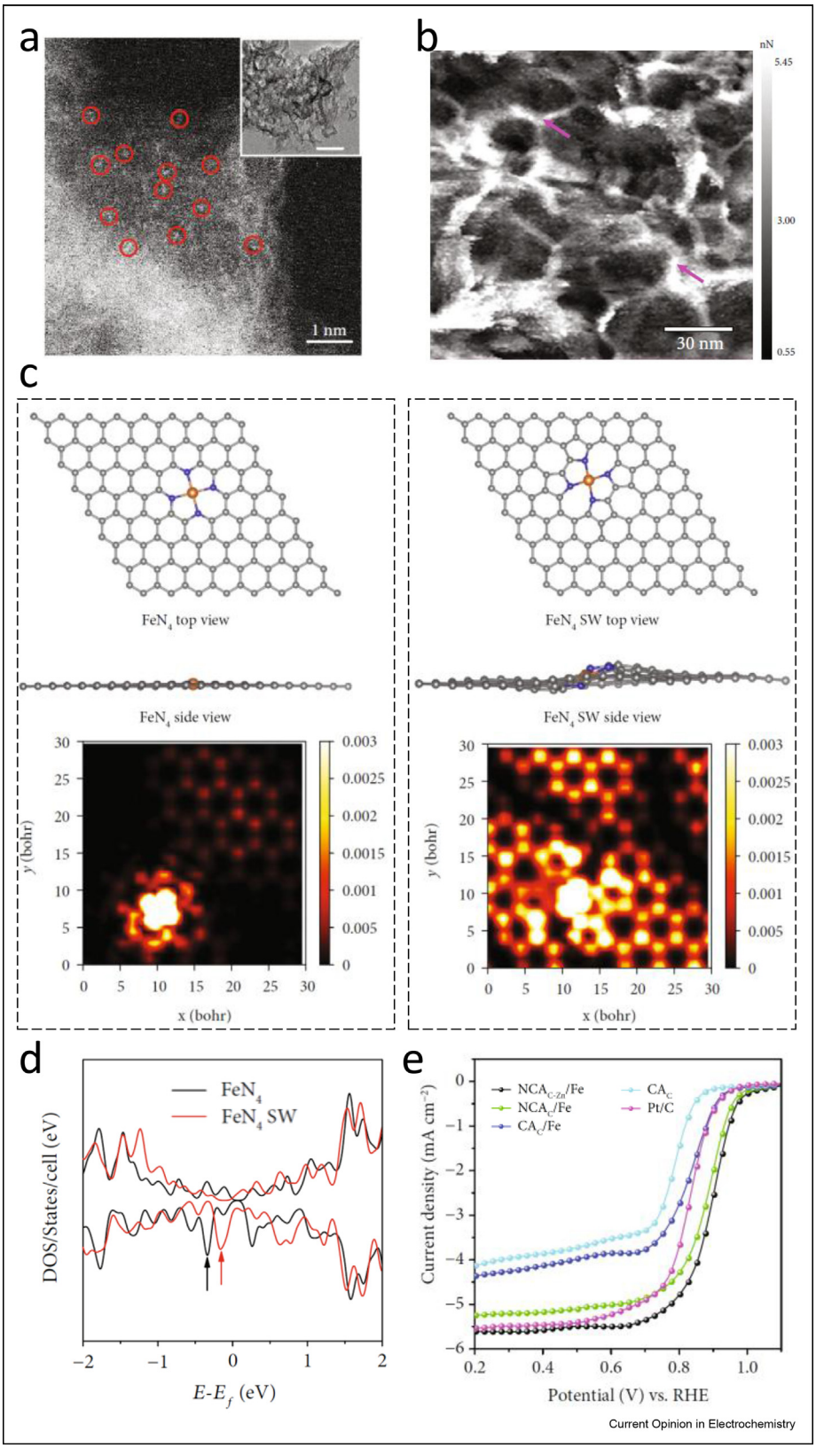

Biomass-derived nanowrinkled carbon aerogels embedded with FeNx moieties. **(a)** Dark-field STEM image of the $NCA_{C\text{-}Zn}$/Fe aerogel. Red circles indicate single Fe atoms. Inset is a TEM image of the $NCA_{C\text{-}Zn}$/Fe aerogel, and the scale bar is 30 nm. **(b)** AFM images of $NCA_{C\text{-}Zn}$/Fe aerogels: adhesion

adjacent N and C sites need to be taken into account in ORR electrocatalysis.

In a more recent study, Zhang et al. [12••] used a polyaniline precursor to prepare pyridine-type FeN_4, which was then converted into pyrrole-type FeN_4 by a pyrolytic treatment with ammonia (Figure 1a), as manifested in soft X-ray absorption spectroscopy (XAS) measurements of the N K-edge and X-ray photoelectron spectroscopy measurements of the N 1s electrons. Such a configurational transformation led to a significant enhancement of the ORR activity, with $E_{1/2}$ increased from +0.71 V to +0.80 V in 0.5 M H_2SO_4 (Figure 1c). Moreover, results from the theoretical study (Figure 1b) showed that the pyrrole-type FeN_4 exhibited a lower overpotential (0.35 eV) from the initial O_2 to H_2O than that of the pyridine-type FeN_4 (0.67 eV) and suppressed the two-electron pathway of H_2O_2. In fact, pyrrole-type FeN_4 exhibited preferred oxygen adsorption with a lower overpotential from O_2 to OOH* than that for the pyridine-type FeN_4.

This argument was further supported in studies with covalent organic frameworks (COFs) derived carbon that contained much better defined coordination of FeN_4, in contrast to traditional pyrolysis that typically generates random configurations of FeN_x. For instance, without any pyrolysis treatment, Peng et al. [23,24] prepared a π-conjugated COF to capture Fe ions in situ forming uniform pyrrole-type FeN_4, used these directly for ORR electrocatalysis, and observed a high $E_{1/2}$ of +0.910 V and enhanced performance as the cathode catalyst for a zinc–air battery, in comparison with commercial Pt/C.

It should be noted that in most of the earlier studies, a two-dimensional planar atomic model is generally assumed for FeN_x, although topological defects are common in pyrolytic carbon. In a latest study, He et al. [14••] prepared nanowrinkled carbon aerogels ($NCA_{C\text{-}Zn}$/Fe) embedded with abundant FeN_x moieties by controlled pyrolysis of biomass-derived hydrogels mixed with Fe and Zn compounds. In Figure 2a, the atomic-scale wrinkled structures (Stone–Wales FeN_4) can be readily identified in the TEM images. In addition, adhesion force measurements (Figure 2b) showed that the winkled structure exhibited a high adhesion force, corresponding to a hydrophilic domain. Fast force mapping measurements suggest that the FeN_4 wrinkled regions also displayed a high electrical conductance. From the simulated STM images (Figure 2c), one can see that the wrinkled Stone–Wales FeN_4 moiety indeed showed a distorted nonplanar structure, in contrast to the normal counterpart. Meanwhile, Figure 2d displays the total density of state of normal and Stone–Wales FeN_4, in which the Fe centers can be found to dominate the contribution to the density of state near the Fermi level, and the marked state of Stone–Wales FeN_4 can be seen to lie closer to the Fermi level than the normal pyridine-type FeN_4, suggesting faster electron transfer of oxygen reduction. This is clearly manifested in electrochemical measurements (Figure 2e).

The results from these studies suggest that nonplanar/distorted carbon skeletons may lead to additional, unique manipulation of the electronic structure and facilitate mass transfer and accessibility of the ORR active sites. In other words, both coordination chemistry and carbon topology are important factors in the rational design and engineering of ORR catalysts.

Cobalt and nitrogen–codoped carbon nanocomposites have also been found to be highly active toward ORR [25–28]. For instance, Yin et al. [26] prepared carbon-supported Co SACs by controlled pyrolysis of zeolitic imidazolate frameworks (ZIFs) at different temperatures and found that CoN_2 exhibited a better ORR activity ($E_{1/2}$ = +0.881 V) than CoN_4 ($E_{1/2}$ = +0.863 V). DFT calculations showed that CoN_2 was more favorable for the four-electron reduction pathway. However, similar to the iron and nitrogen–codoped carbon nanocomposites, in most studies, CoN_4 is the leading coordination structure proposed to be the ORR active sites. For instance, Wan et al. [29•] prepared a cobalt and nitrogen–codoped carbon nanocomposite by pyrolysis of a cobalt complex (Figure 3a) and ascribed the high ORR activity ($E_{1/2}$ = +0.85 V) and anti-poisoning ability in alkaline, but not in acidic, media (Figure 3b and c) to the formation of CoN_4 configurations in the final product (CoNC). They argued that the pyridinic N sites neighboring the Co center served as the main active sites when SCN^- was bound to Co in alkaline, but not in acidic, media. Cheng et al. [28] also found that CoN_4 exhibited better resistance against SCN^- poisoning than FeN_4, which is consistent with the results from DFT calculations that O_2 increased the stability of CoN_4 but not for FeN_4. It should be noted that although CoN_4 has been recognized as the ORR active moiety in most studies, further research is desired to unravel the mechanistic correlation of the CoN_x atomic configuration with the ORR activity.

Copper and nitrogen–codoped carbon nanocomposites have also emerged recently as promising ORR catalysts in alkaline media, with a performance comparable to that of state-of-the-art FeN_x [11,19,30–32]. For instance, Li et al. [11] synthesized a CuN_x SAC via

force image. **(c)** Side/top view and simulated STM image (at a bias of −1.0 V) of normal FeN_4 and FeN_4 SW-doped graphene sheets. **(d)** Density of state (DOS) of normal FeN_4 and FeN_4 SW-doped graphene sheets. **(e)** ORR polarization curves of CA_C, CA_C/Fe, NCA_C/Fe, and $NCA_{C\text{-}Zn}$/Fe, as well as Pt/C, at 1600 rpm in 0.1 M KOH at the potential sweep rate of 5 mV s^{-1}. Reprinted with permission from He et al. [14••] © 2019 the authors. ORR, oxygen reduction reaction; STEM, scanning transmission electron microscopy; TEM, transmission electron microscopy; STM, scanning tunneling microscopy; AFM, atomic force microscopy; RHE, reversible hydrogen electrode; SW, Stone-Wales; CA_C, carbon aerogel derived from chitosan; NCA_C, nitrogen-doped carbon aerogel derived from chitosan.

Figure 3

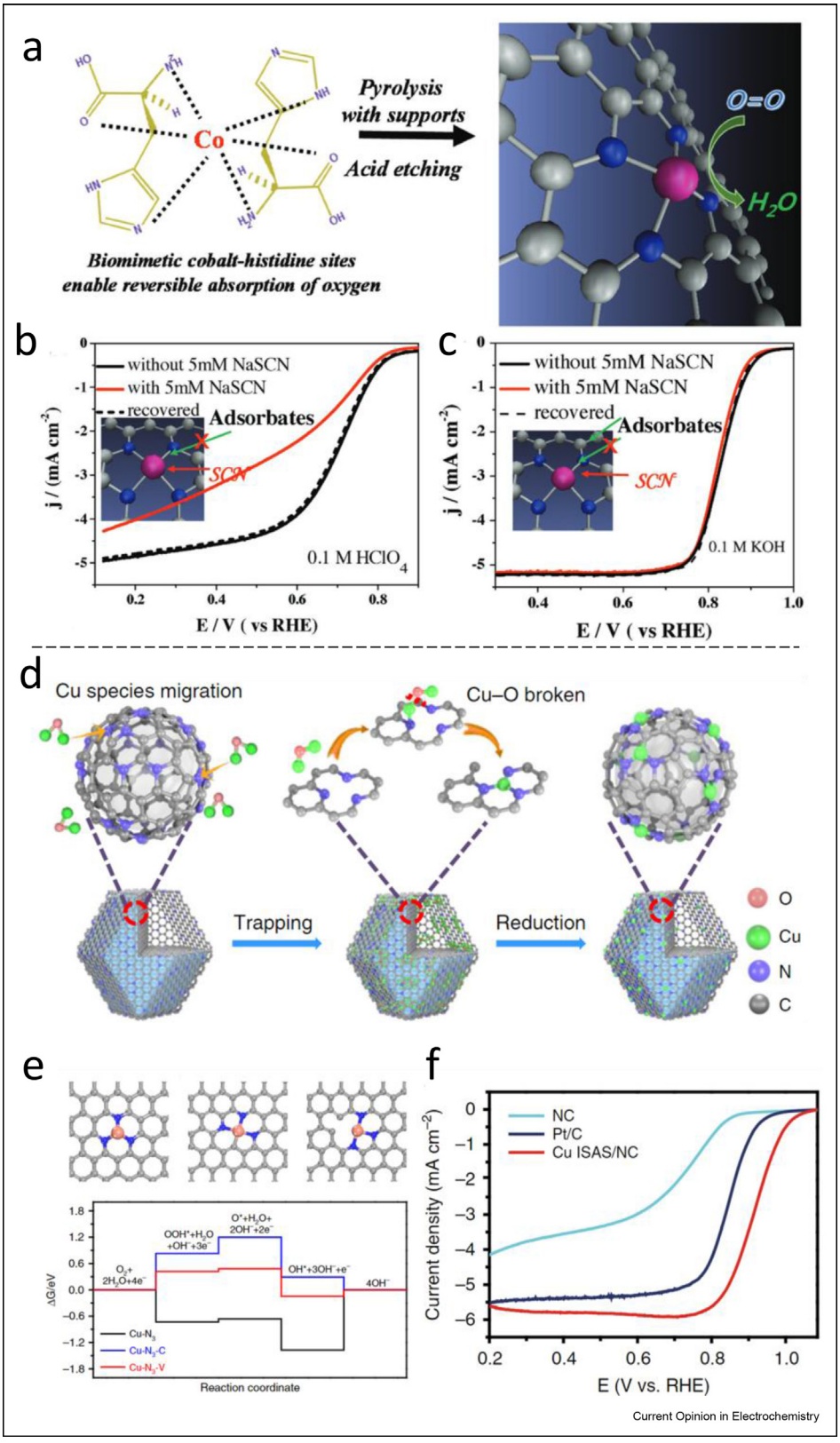

Co and Cu single atom catalysts for ORR electrocatalysis. **(a)** Schematic illustration of the support-assisted pyrolysis synthesis of CoNC catalysts. LSV curves of CoNC with and without 5 mM NaSCN in **(b)** acidic and **(c)** alkaline media. Reprinted with permission from Wan et al. [29•] © 2018 Wiley-VCH. **(d)** Scheme of the formation of isolated copper sites (Cu ISAS/N–C) catalyst. **(e)** Free energy diagram for ORR process on these three models at the equilibrium potential (U = +0.40 V vs. NHE or U = +1.23 V vs RHE) at pH = 14. **(f)** LSV curves of NC, Cu ISAS/NC, and Pt/C catalysts in 0.1 M KOH solution at the sweep rate of 10 mV s^{-1} and rotation rate of 1600 rpm. Reprinted with permission from Yang et al. [19•] © 2019 Macmillan Publishers Limited. LSV, linear sweep voltammetry; ORR, oxygen reduction reaction; RHE, reversible hydrogen electrode; ISAS, isolated single atom site.

Figure 4

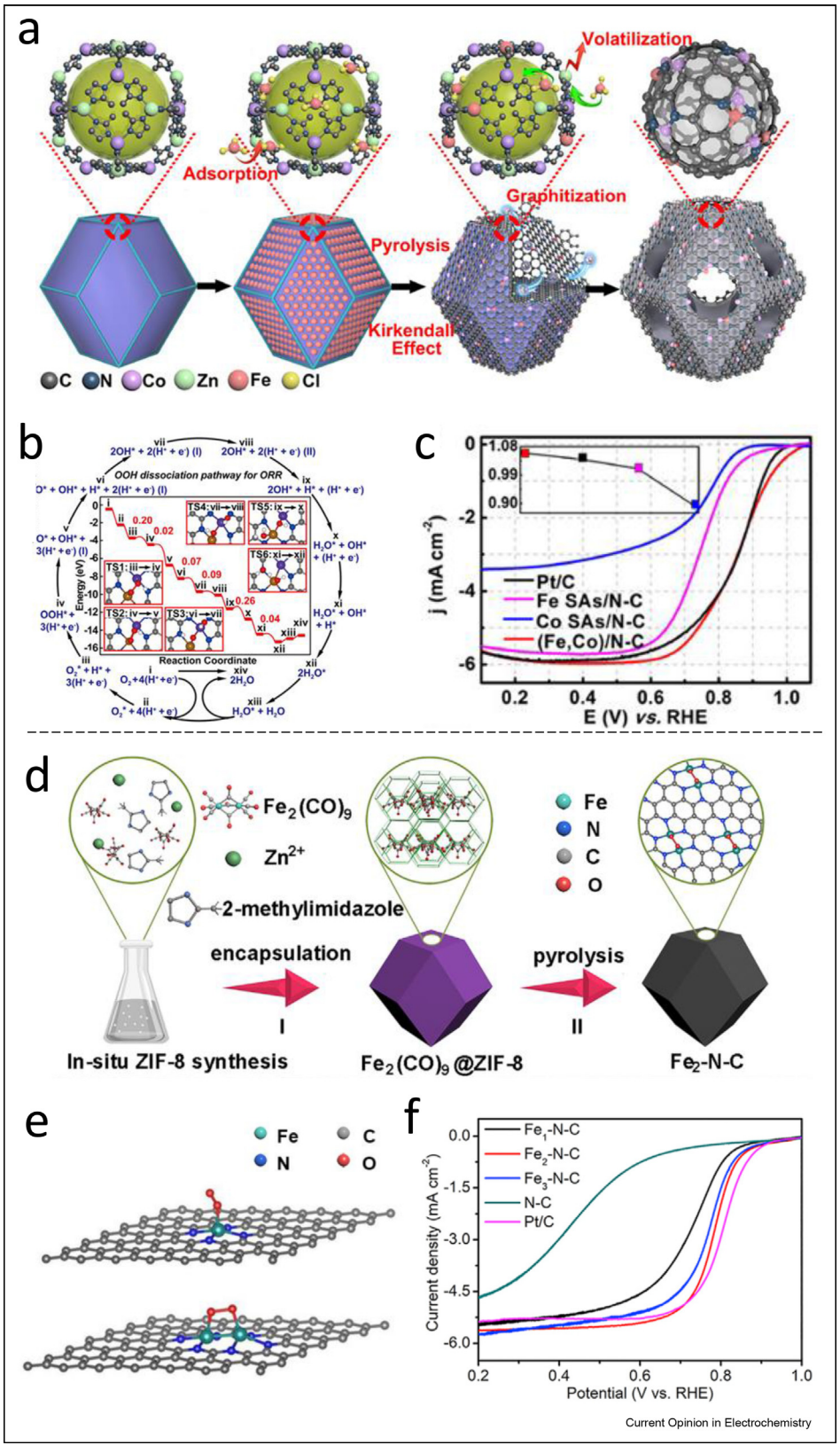

Multinuclear metal sites for ORR electrocatalysis. **(a)** Preparation of (Fe,Co)/N–C. **(b)** Energies of intermediates and transition states in mechanism of ORR at (Fe,Co)/N–C from DFT. **(c)** RDE polarization curves of Pt/C, Co SAs/N–C, Fe SAs/N–C, and (Fe,Co)/N–C in O_2-saturated 0.1 M $HClO_4$ with a

pyrolysis and the acid-leaching method, which outperformed Pt/C in alkaline media toward ORR with an $E_{1/2}$ of +0.865 V. XAS fitting analysis showed a mixed structure of CuN_4 and CuN_2 (without C coordination), and the latter exhibited a more favorable adsorption affinity to O_2 and OOH than the former. The conclusion is consistent with the results from a former study by Wu et al. [30] that CuN_2 ($E_{1/2}$ = +0.80 V in alkaline media) was the apex among the series of CuN_x configurations. Another study by Yang et al. [19•] suggested that defected structures such as CuN_3—V (vacancy, without C coordination, Figure 3e) might account for the remarkable ORR activity as well. As shown in Figure 3d, when Cu(I)O was evaporated onto the defect-rich carbon skeleton derived pyrolytically from ZIF-8, the obtained CuN_x nanocomposites reached a record high $E_{1/2}$ of +0.92 V in alkaline media (Figure 3f). Theoretical calculations in Figure 3e showed that the formation of OOH* was the RDS of the CuN_3—V and CuN_3—C structures and the removal of OH* is the RDS of CuN_3. Moreover, the vacancy defect of CuN_3—V was argued to decrease the theoretical ORR overpotential (0.42 eV) which was much lower than that of CuN_3—C (0.83 eV) and CuN_3 (1.37 eV). It is interesting to see that with N-doped graphene or carbon nanotubes neither of the Cu single atoms exhibited good ORR activity. This suggests that the introduction of structural defects (vacancies) into the CuN_x moiety may be a promising way to manipulate and enhance the ORR activity.

Besides Fe, Co, and Cu, other metal and nitrogen—codoped carbon nanocomposites, such as Ni [33], Zn [34,35], and Cr [36], have also been prepared and shown apparent ORR activity. For example, Li et al. [34] slowly annealed ZIF-8 powers (at the heating rate of 1 °C min^{-1}) to produce carbon embedded with ZnN_4, which exhibited an ultrahigh loading of 9.33 wt% Zn and an $E_{1/2}$ of +0.873 V toward ORR in 0.1 M KOH. The performance was slightly subpar compared with that of the FeN_x counterparts prepared in the same fashion, and DFT calculations showed that ZnN_4 was more stable than FeN_4 and hence was less active in binding oxygen intermediates. In another study, Luo et al. [36] pyrolyzed Cr^{3+}-soaked ZIF-8 and successfully prepared CrN_4-doped carbon, which exhibited an $E_{1/2}$ of +0.773 V in acid. In comparison with FeN_4, CrN_4 showed superb durability of ORR activity, showing only a 15 mV decrease of $E_{1/2}$ after 20,000 cyclic voltammetric cycles.

It should be noted that most metal and nitrogen—codoped carbon hybrids demonstrate remarkable ORR activity in alkaline media, but the activity deteriorates markedly in acidic media. In a recent study, Dong et al. [37] demonstrated that the assistance of a neighboring metal site led to a significant improvement of the ORR activity in acid. This suggests that structural engineering of dinuclear moieties ($M_1M_2N_x$) may be an effective strategy to extend the applications of carbon-based SACs to ORR in acid. For instance, Wang et al. [38••] used a host—guest strategy (Figure 4a) to construct Fe—Co coupling sites in N-doped carbon, and the resulting dinuclear catalyst showed an $E_{1/2}$ of +0.863 V in 0.1 M $HClO_4$, a performance much better than that of FeN_x and CoN_x (Figure 4c). DFT calculations of the N_3—Fe—Co—N_3 model (Figure 4b) showed that the dissociation barrier of O_2, OOH on Fe—Co dual sites, was much lower than that with FeN_x and CoN_x alone. In addition, the calculations showed that the bridge-like adsorption of O_2 molecules was facilitated on the Fe—Co dinuclear sites, which led to enhanced dissociation of the O atoms and the four-electron reduction pathway.

In another study, Ye et al. [39•] also showed that dual metal sites facilitated ORR electrocatalysis in acid. Experimentally, three iron precursors, monomeric $Fe(acac)_2$, dimeric $Fe_2(CO)_9$, and trimeric $Fe_3(CO)_{12}$, were encapsulated by ZIF-8, which was then pyrolyzed, resulting in the formation of iron and nitrogen—codoped carbon that exhibited individual Fe centers (Fe_1—N—C), dinuclear sites (Fe_2—N—C), and trinuclear sites (Fe_3—N—C) (Figure 4d). The Fe_2—N—C sample was found to demonstrate an $E_{1/2}$ of +0.78 V that was better than that of Fe_1—N—C (+0.715 V) and Fe_3—N—C (+0.762 V) (Figure 4f). The results of low-temperature infrared spectroscopic measurements showed that the number of the Fe sites influenced the adsorption of O_2. As shown in Figure 4e, Fe_1—N—C mainly entailed superoxide-like adsorption of O_2 molecules, whereas the peroxide-like mode was observed with Fe_2—N—C and Fe_3—N—C. The bridge-like adsorption mode in the latter was beneficial for the cleavage of O_2 owing to the elongation of the O—O bonds.

Alkaline ORR electrocatalysis can also be enhanced with a dinuclear configuration by taking advantage of the electronic coupling between the metal centers, analogous to that in alloy nanoparticles [40—45]. There are several critical challenges in these studies. The first is to develop effective synthetic protocols to prepare dinuclear atom catalysts. Second, it is critical to quantify the atomic configurations of the metal centers, in particular, the electronic interactions between the two metal sites. In addition to XAS, other techniques, such as subangstrom electron energy loss spectroscopic (EELS) mapping and in situ Raman spectroscopy, are highly desired

sweep rate of 10 mV s^{-1} and a rotation rate of 1600 rpm. Inset: E_{onset} of different catalysts. Reprinted with permission from Wang et al. [38••] © 2017 American Chemical Society. **(d)** Schematic illustration for the two-step synthesis of Fe_2–N–C. Step I: in situ encapsulation of $Fe_2(CO)_9$ in the cavity of ZIF-8 to form $Fe_2(CO)_9$@ZIF-8. Step II: high-temperature pyrolysis to obtain Fe_2 cluster anchored on N-doped carbon. **(e)** Adsorption modes of O_2 on Fe_1–N–C and Fe_2–N–C. **(f)** ORR polarization curves in O_2-saturated 0.5 M H_2SO_4 solution at a sweep rate of 10 mV s^{-1} and a rotation speed of 1600 rpm. Reprinted with permission from Ye et al. [39•] © 2019 Elsevier Ltd. ORR, oxygen reduction reaction; ZIF, zeolitic imidazolate framework; DFT, density functional theory; RDE, rotating disk electrode.

to resolve the fine structures of the dinuclear $M_1M_2N_xC_y$ moiety. In conjunction with DFT studies, the mechanistic insights can then be unraveled, an important step toward rational design and engineering of ORR catalysts in both acidic and alkaline media.

In summary, recently there has been substantial progress in the design and engineering of metal–nitrogen coordination moieties in carbon for ORR electrocatalysis. Mechanistically, the incorporation of select metal centers within the carbon scaffolds in the form of M–N bonds leads to activation of multiple atomic sites in close proximity, which collectively contribute to the ORR activity. Thus, the exact atomic configuration is found to play a key role in determining the adsorption of critical reaction intermediates and the eventual catalytic performance. Furthermore, recent studies have shown that the carbon topological defects are another important variable that can be exploited for further enhancement of the electrocatalytic activity, in particular, to develop SACs that are selective for the four-electron oxygen reduction pathway.

It should be recognized that despite the progress, it remains challenging to unify the mechanistic accounts for the ORR activity. In fact, one can see that there exists apparent discrepancy among leading studies in the literature. This is primarily because most carbon SACs are prepared pyrolytically and exhibit structural complexity, and the nonuniformity within even the same batch of sample further compounds the issue, whereas in theoretical modeling, the structures are highly simplified and short-ranged. This inevitably creates a gap between the theoretical model and the actual structure, raising questions about the validity of the identification of the ORR active sites by a correlation between the experimental work and theoretical modeling and simulations. An immediate question arises. Is it possible to develop *de novo* bottom-up approaches to the fabrication of carbon-based SACs? It will no doubt be a daunting undertaking. Yet the well-defined structures will allow for a reliable correlation between experiment and theory. Furthermore, extensive progress in organometallic chemistry can be exploited to extend the study to a wide range of coordination chemistry, within the context of metal centers, coordinating ligands, metal–ligand charge transfer, metal–metal charge transfer, and so on. Furthermore, to aid in the unraveling of the fundamental mechanisms of catalytic reactions, development of effective tools for in situ spectroscopic/microscopic measurements is equally important. Some of these are actually being pursued.

Acknowledgements

This work was supported in part by the National Science Foundation (CHE-1710408 and CHE-1900235). QxL acknowledges a research fellowship from the Shanghai Municipal Education Commission.

References

Papers of particular interest, published within the period of review, have been highlighted as:

- • of special interest
- •• of outstanding interest

1. Seh ZW, Kibsgaard J, Dickens CF, Chorkendorff IB, Norskov JK, Jaramillo TF: **Combining theory and experiment in electrocatalysis: insights into materials design**. *Science* 2017, **355**, eaad4998.

2. Peng Y, Lu BZ, Chen SW: **Carbon-supported single atom catalysts for electrochemical energy conversion and storage**. *Adv Mater* 2018, **30**:1801995.

3. Xiong Y, Yang Y, DiSalvo FJ, Abruna HD: **Metal-organic-framework-derived Co-Fe bimetallic oxygen reduction electrocatalysts for alkaline fuel cells**. *J Am Chem Soc* 2019, **141**: 10744–10750.

4. Ren H, Wang Y, Yang Y, Tang X, Peng YQ, Peng HQ, Xiao L, Lu JT, Abruna HD, Zhuang L: **Fe/N/C nanotubes with atomic Fe sites: a highly active cathode catalyst for alkaline polymer electrolyte fuel cells**. *ACS Catal* 2017, **7**:6485–6492.

5. Peng Y, Lu BZ, Wang N, Lu JE, Li CH, Ping Y, Chen SW: **Oxygen reduction reaction catalyzed by black-phosphorus-supported metal nanoparticles: impacts of interfacial charge transfer**. *ACS Appl Mater Interfaces* 2019, **11**:24707–24714.

6. Liu MM, Wang LL, Zhao KN, Shi SS, Shao QS, Zhang L, Sun XL, Zhao YF, Zhang JJ: **Atomically dispersed metal catalysts for the oxygen reduction reaction: synthesis, characterization, reaction mechanisms and electrochemical energy applications**. *Energy Environ Sci* 2019, **12**:2890–2923.

7. Deng J, Ren PJ, Deng DH, Bao XH: **Enhanced electron penetration through an ultrathin graphene layer for highly efficient catalysis of the hydrogen evolution reaction**. *Angew Chem Int Ed* 2015, **54**:2100–2104.

8. Li Y, Liu X, Zheng L, Shang J-X, Wan X, Hu R, Guo X, Hong S, Shui J: **Preparation of Fe-NC catalysts with FeNx (x= 1, 3, 4) active sites and comparison of their activities for oxygen reduction reaction and performances in proton exchange membrane fuel cell**. *J Mater Chem A* 2019, **7**:26147–26153.

9. Shen HJ, Gracia-Espino E, Ma JY, Tang HD, Mamat X, Wagberg T, Hu GZ, Guo SJ: **Atomically FeN2 moieties dispersed on mesoporous carbon: a new atomic catalyst for efficient oxygen reduction catalysis**. *Nano Energy* 2017, **35**: 9–16.

10. Zhu CZ, Shi QR, Xu BZ, Fu SF, Wan G, Yang C, Yao SY, Song JH, Zhou H, Du D, *et al.*: **Hierarchically porous M-N-C (M = Co and Fe) single-atom electrocatalysts with robust MNx active moieties enable enhanced ORR performance**. *Adv Energy Mater* 2018, **8**:1801956.

11. Li F, Han GF, Noh HJ, Kim SJ, Lu YL, Jeong HY, Fu ZP, Baek JB: **Boosting oxygen reduction catalysis with abundant copper single atom active sites**. *Energy Environ Sci* 2018, **11**: 2263–2269.

12. •• Zhang N, Zhou T, Chen M, Feng H, Yuan R, Yan W, Tian Y-C, Wu X, Chu W, Wu C: **High-purity pyrrole-type FeN4 site as superior oxygen reduction electrocatalyst**. *Energy Environ Sci* 2020, https://doi.org/10.1039/C1039EE03027A.
Pyrrole-type FeN_4 exhibits a better ORR performance than the pyridine-type both in experimental measurements and in DFT calculations.

13. Lu BZ, Smart TJ, Qin DD, Lu JE, Wang N, Chen LM, Peng Y, Ping Y, Chen SW: **Nitrogen and iron-codoped carbon hollow nanotubules as high-performance catalysts toward oxygen reduction reaction: a combined experimental and theoretical study**. *Chem Mater* 2017, **29**:5617–5628.

14. •• He T, Lu B, Chen Y, Wang Y, Zhang Y, Davenport JL, Chen AP, Pao C-W, Liu M, Sun Z, *et al.*: **Nanowrinkled carbon aerogels embedded with FeNx sites as effective oxygen electrodes for rechargeable zinc-air battery**. *Research* 2019. https://spj.sciencemag.org/research/aip/6813585/Distorted Stone-Wales; 2019.
FeN_4 loaded on nanowrinkled N-doped carbon outperforms commercial Pt/C towards ORR in alkaline media.

15. Fu XG, Li N, Ren BH, Jiang GP, Liu YR, Hassan FM, Su D, Zhu JB, Yang L, Bai ZY, *et al.*: **Tailoring FeN4 sites with edge**

enrichment for boosted oxygen reduction performance in proton exchange membrane fuel cell. *Adv Energy Mater* 2019, **9**:1803737.

16. Jiang R, Li L, Sheng T, Hu GF, Chen YG, Wang LY: **Edge-site engineering of atomically dispersed Fe-N-4 by selective C-N bond cleavage for enhanced oxygen reduction reaction activities**. *J Am Chem Soc* 2018, **140**:11594–11598.

17. Workman MJ, Serov A, Tsui LK, Atanassov P, Artyushkova K: **Fe-N-C catalyst graphitic layer structure and fuel cell performance**. *ACS Energy Lett* 2017, **2**:1489–1493.

18. Lee SH, Kim J, Chung DY, Yoo JM, Lee HS, Kim MJ, Mun BS, Kwon SG, Sung YE, Hyeon T: **Design principle of Fe-N-C electrocatalysts: how to optimize multimodal porous structures?** *J Am Chem Soc* 2019, **141**:2035–2045.

19. • Yang ZK, Chen BX, Chen WX, Qu YT, Zhou FY, Zhao CM, Xu Q, Zhang QH, Duan XZ, Wu Y: **Directly transforming copper (I) oxide bulk into isolated single-atom copper sites catalyst through gas-transport approach**. *Nat Commun* 2019, **10**:3734.
Cu-N_x-C exhibits a higher ORR activity than commercial Pt/C in alkaline media, where the defective Cu–N_3–V is argued to be the active site.

20. Yang L, Cheng DJ, Zeng XF, Wan X, Shui JL, Xiang ZH, Cao DP: **Unveiling the high-activity origin of single-atom iron catalysts for oxygen reduction reaction**. *Proc Natl Acad Sci USA* 2018, **115**:6626–6631.

21. Chen YJ, Ji SF, Wang YG, Dong JC, Chen WX, Li Z, Shen RA, Zheng LR, Zhuang ZB, Wang DS, *et al.*: **Isolated single iron atoms anchored on N-doped porous carbon as an efficient electrocatalyst for the oxygen reduction reaction**. *Angew Chem Int Ed* 2017, **56**:6937–6941.

22. He T, Zhang YQ, Chen Y, Zhang ZZ, Wang HY, Hu YF, Liu M, Pao CW, Chen JL, Chang LY, *et al.*: **Single iron atoms stabilized by microporous defects of biomass-derived carbon aerogels as high-performance cathode electrocatalysts for aluminum-air batteries**. *J Mater Chem A* 2019, **7**:20840–20846.

23. Peng P, Shi L, Huo F, Mi CX, Wu XH, Zhang SJ, Xiang ZH: **A pyrolysis-free path toward superiorly catalytic nitrogen-coordinated single atom**. *Sci Adv* 2019, **5**. eaaw2322.

24. Peng P, Shi L, Huo F, Zhang S, Mi C, Cheng Y, Xiang Z: **In situ charge exfoliated soluble covalent organic framework directly used for Zn-air flow battery**. *ACS Nano* 2019, **13**:878–884.

25. Han YH, Wang YG, Chen WX, Xu RR, Zheng LR, Zhang J, Luo J, Shen RA, Zhu YQ, Cheong WC, *et al.*: **Hollow N-doped carbon spheres with isolated cobalt single atomic sites: superior electrocatalysts for oxygen reduction**. *J Am Chem Soc* 2017, **139**:17269–17272.

26. Yin PQ, Yao T, Wu Y, Zheng LR, Lin Y, Liu W, Ju HX, Zhu JF, Hong X, Deng ZX, *et al.*: **Single cobalt atoms with precise N-coordination as superior oxygen reduction reaction catalysts**. *Angew Chem Int Ed* 2016, **55**:10800–10805.

27. Sun TT, Zhao S, Chen WX, Zhai D, Dong JC, Wang Y, Zhang SL, Han AJ, Gu L, Yu R, *et al.*: **Single-atomic cobalt sites embedded in hierarchically ordered porous nitrogen-doped carbon as a superior bifunctional electrocatalyst**. *Proc Natl Acad Sci USA* 2018, **115**:12692–12697.

28. Cheng QQ, Yang LJ, Zou LL, Zou ZQ, Chen C, Hu Z, Yang H: **Single cobalt atom and N codoped carbon nanofibers as highly durable electrocatalyst for oxygen reduction reaction**. *ACS Catal* 2017, **7**:6864–6871.

29. • Wan G, Yu PF, Chen HR, Wen JG, Sun CJ, Zhou H, Zhang N, Li QR, Zhao WP, Xie B, *et al.*: **Engineering single-atom cobalt catalysts toward improved electrocatalysis**. *Small* 2018, **14**:1704319.
Co–N–C is poisoned by SCN^- in acid but not in alkaline media. Poisoning test is an efficient way to identify the ORR active site of Co–N–C.

30. Wu HH, Li HB, Zhao XF, Liu QF, Wang J, Xiao JP, Xie SH, Si R, Yang F, Miao S, *et al.*: **Highly doped and exposed Cu(I)-N active sites within graphene towards efficient oxygen reduction for zinc-air batteries**. *Energy Environ Sci* 2016, **9**:3736–3745.

31. Wang DH, Ao CC, Liu XK, Fang S, Lin Y, Liu W, Zhang W, Zheng XS, Zhang LD, Yao T: **Coordination-engineered Cu-N-x single-site catalyst for enhancing oxygen reduction reaction**. *ACS Appl Energy Mater* 2019, **2**:6497–6504.

32. Qu YT, Li ZJ, Chen WX, Lin Y, Yuan TW, Yang ZK, Zhao CM, Wang J, Zhao C, Wang X, *et al.*: **Direct transformation of bulk copper into copper single sites via emitting and trapping of atoms**. *Nat Catal* 2018, **1**:781–786.

33. Fei HL, Dong JC, Feng YX, Allen CS, Wan CZ, Volosskiy B, Li MF, Zhao ZP, Wang YL, Sun HT, *et al.*: **General synthesis and definitive structural identification of MN4C4 single-atom catalysts with tunable electrocatalytic activities**. *Nat Catal* 2018, **1**:63–72.

34. Li J, Chen SG, Yang N, Deng MM, Ibraheem S, Deng JH, Li J, Li L, Wei ZD: **Ultrahigh-loading zinc single-atom catalyst for highly efficient oxygen reduction in both acidic and alkaline media**. *Angew Chem Int Ed* 2019, **58**:7035–7039.

35. Song P, Luo M, Liu XZ, Xing W, Xu WL, Jiang Z, Gu L: **Zn single atom catalyst for highly efficient oxygen reduction reaction**. *Adv Funct Mater* 2017, **27**:1700802.

36. Luo EG, Zhang H, Wang X, Gao LQ, Gong LY, Zhao T, Jin Z, Ge JJ, Jiang Z, Liu CP, *et al.*: **Single-atom Cr-N-4 sites designed for durable oxygen reduction catalysis in acid media**. *Angew Chem Int Ed* 2019, **58**:12469–12475.

37. Dong JC, Zhang XG, Briega-Martos V, Jin X, Yang J, Chen S, Yang ZL, Wu DY, Feliu JM, Williams CT, *et al.*: **In situ Raman spectroscopic evidence for oxygen reduction reaction intermediates at platinum single-crystal surfaces**. *Nat Energy* 2019, **4**:60–67.

38. •• Wang J, Huang ZQ, Liu W, Chang CR, Tang HL, Li ZJ, Chen WX, Jia CJ, Yao T, Wei SQ, *et al.*: **Design of N-coordinated dual-metal sites: a stable and active Pt-free catalyst for acidic oxygen reduction reaction**. *J Am Chem Soc* 2017, **139**:17281–17284.
Dual Co sites embedded in N-doped carbon provide efficient active sites towards ORR in acid, with a performance comparable to that of commercial Pt/C and better than that of Fe SAC and Co SAC.

39. • Ye W, Chen S, Lin Y, Yang L, Chen S, Zheng X, Qi Z, Wang C, Long R, Chen M: **Precisely tuning the number of Fe atoms in clusters on N-doped carbon toward acidic oxygen reduction reaction**. *Chem* 2019, **5**:2865–2878.
Dual metal sites in Fe2–N–C allow for a bridge-like adsorption of O2, which is more beneficial for the dissociation of the intermediates than the single-atom Fe1–N–C.

40. Zhang DY, Chen WX, Li Z, Chen YJ, Zheng LR, Gong Y, Li QH, Shen RA, Han YH, Cheong WC, *et al.*: **Isolated Fe and Co dual active sites on nitrogen-doped carbon for a highly efficient oxygen reduction reaction**. *Chem Commun* 2018, **54**:4274–4277.

41. Gong SP, Wang CL, Jiang P, Hu L, Lei H, Chen QW: **Designing highly efficient dual-metal single-atom electrocatalysts for the oxygen reduction reaction inspired by biological enzyme systems**. *J Mater Chem A* 2018, **6**:13254–13262.

42. Wang BW, Zou JX, Shen XC, Yang YC, Hu GZ, Li W, Peng ZM, Banham D, Dong AG, Zhao DY: **Nanocrystal supracrystal-derived atomically dispersed Mn-Fe catalysts with enhanced oxygen reduction activity**. *Nano Energy* 2019, **63**:103851.

43. Zhang LZ, Fischer JMTA, Jia Y, Yan XC, Xu W, Wang XY, Chen J, Yang DJ, Liu HW, Zhuang LZ, *et al.*: **Coordination of atomic Co-Pt coupling species at carbon defects as active sites for oxygen reduction reaction**. *J Am Chem Soc* 2018, **140**:10757–10763.

44. Lu ZY, Wang BF, Hu YF, Liu W, Zhao YF, Yang RO, Li ZP, Luo J, Chi B, Jiang Z, *et al.*: **An isolated zinc-cobalt atomic pair for highly active and durable oxygen reduction**. *Angew Chem Int Ed* 2019, **58**:2622–2626.

45. Han XP, Ling XF, Yu DS, Xie DY, Li LL, Peng SJ, Zhong C, Zhao NQ, Deng YD, Hu WB: **Atomically dispersed binary Co-Ni sites in nitrogen-doped hollow carbon nanocubes for reversible oxygen reduction and evolution**. *Adv Mater* 2019:1905622.